Quantum hydrodynamic modeling of edge modes in chiral Berry plasmons

Ya Zhang,[1] Feng Zhai,[2] Bin Guo,[1,*] Lin Yi,[3] and Wei Jiang[3,†]
[1]*Department of Physics, Wuhan University of Technology, Wuhan 430070, China*
[2]*Department of Physics, Zhejiang Normal University, Zhejiang 321004, China*
[3]*School of Physics, Huazhong University of Science and Technology, Wuhan 430074, China*
(Received 9 February 2017; revised manuscript received 20 June 2017; published 5 July 2017)

A quantum hydrodynamic model is used to study the edge modes of chiral Berry plasmons in two-dimensional materials with nonzero Berry flux. A quantum effect of collective electron motions appears in systems with a high electron density. For the considered edge plasmon, the transcendental equation of the dispersion relation is solved nonlinearly and semianalytically. We predict a one-way chiral edge state in the presence of the quantum statistical effect and quantum diffraction effect. Indeed, the plasmon frequencies for counterpropagating edge modes exhibit different long-wavelength limits. The quantum effect can enhance the chirality of edge plasmons and their spatial confinement.

DOI: 10.1103/PhysRevB.96.045104

I. INTRODUCTION

Edge plasmons were first discovered in a two-dimensional electron gas (2DEG) system confined in a liquid-helium surface [1,2] and under magnetic fields. For edge magnetoplasmons (MPs), Aleiner and Glazman have found a new acoustic edge mode of a 2D electron liquid [3]. Resonant edge MPs in graphene have been investigated by high-frequency electronic measurements [4], promoting the use of graphene for quantum transport experiments and plasmonic applications. Recently, Jin *et al.* [5] have revealed the topological origin of edge MPs and predicted a new type of one-way edge MP in a 2DEG system modulated by opposite magnetic domains. Topological plasmons have also been predicted in metallic nanoparticles [6], which are relevant for manipulating light at the nanoscale.

Edge plasmons without magnetic field have been reported in graphene systems. In patterned graphene nanoribbons fabricated with high-quality chemical-vapor-deposited graphene on Al_2O_3 substrates, peculiar one-dimensional modes propagating along the edges have been observed experimentally [7]. In graphene disks and rectangular nanoresonators, a near-field optical experiment [8] has justified the larger confinements of the edge modes compared to surface plasmons, which could have potential applications in the development of highly sensitive spectroscopy and detection [9]. Strain in graphene films acts as a pseudomagnetic field which has opposite signs for electrons from different valleys. For strained graphene with time-reversal symmetry, Principi *et al.* [10] have predicted that two charged counterpropagating acoustic edge modes exist at the boundary.

In gapped graphene and transition-metal dichalcogenide monolayers, there exists a finite net Berry flux when the Fermi energy lies in the conduction or valence band [11,12]. For 2DEG systems with nonzero Berry flux, Song *et al.* [13] have reported theoretically that counterpropagating charge density waves exist on the boundary and exhibit split energy dispersions. These edge plasmon acoustic modes are regarded as chiral Berry plasmons (CBPs) [13]. In gapped graphene with Fermi energy inside the band gap, a pumping with circularly polarized light can generate a net Berry flux and thus CBPs [14]. Chiral edge plasmons in the absence of magnetic field are appealing for realizing optical nonreciprocity at the subwavelength scale [15,16].

In a high-density 2DEG, a quantum effect (QE) of collective electron motions is expected to appear. One basic collective property of a plasma is the tendency for quasineutrality due to the shielding of any excess charge in the system. It is evident that the shielding is a collective effect due to a large number of particles surrounding the charged particle. Haas has predicted that the classical screening effect still holds in the quantum (degenerate) case, with the replacement $k_BT \rightarrow E_F$ (thermal energy $\rightarrow$ Fermi energy) [17]. In a 2DEG, the shielding length is $\lambda_F = (2\pi n_0)^{(-1/2)}$, which is not zero even at zero temperature due to the Pauli exclusion principle, compared to a classical plasma. The collective effects are important in quantum plasmas when the characteristic size of the system $L \gg \lambda_F$. Therefore, for a dense plasma, the collective effects (quantum effects of the collective motion) become important. There has been great interest in the study of collective plasma modes with QE [18–21]. Haas *et al.* have introduced the quantum hydrodynamic (QHD) theory based on the nonlinear Schrödinger-Poisson or Wigner-Poisson kinetic models [18,19]. It has been reported that QEs can stabilize a classically unstable mode, while sufficiently large QEs tend to suppress the instability [20]. The reason is that the QE inhibits the spreading of energy among different waves. Marklund *et al.* have predicted a quantum spin effect on the dispersion relation of a linear wave in plasmas with high densities [21]. Very recently, the QE on an ion stopping power of dense plasmas has been reported experimentally [22].

In this paper, we examine the QE on a dispersive relation and the transverse confinement of edge plasmons propagating along the boundary of a 2DEG with nonzero Berry flux. By solving the QHD model coupled with the anomalous velocity induced by the Berry curvature, we find that in the presence of QE, acoustic edge plasmons propagate unidirectionally. This result is in contrast to that of Ref. [13], where frequencies for oppositely directed edge modes exhibit symmetric long-wavelength limits. Under the QE, the plasmon frequencies for counterpropagating edge modes exhibit different

*binguo@whut.edu.cn
†weijiang@hust.edu.cn

long-wavelength limits. In addition, for the edge plasmon modes, the QE can also generate direction-dependent frequency gaps and enhance transverse confinement. The outline of the paper is as follows. Section II presents the QHD model to describe chiral Berry plasmons with a finite Berry flux. In Sec. III, we derive the dispersion relation for the edge plasmon and give the long-wavelength limits of oppositely directed edge modes. In Sec. IV, the nonlinear and semianalytical results of the dispersion relation and the transverse confinement are shown and discussed. In Sec. V, the experimental realization of these theoretical results is briefly discussed. Finally, a short conclusion is made in Sec. VI.

II. QUANTUM HYDRODYNAMIC MODEL

The system under consideration is a 2DEG in an (x,y) plane with a finite Berry flux. Candidate materials include 2D gapped Dirac materials such as graphene and transition-metal dichalcogenide monolayers [11,12]. Similar to Refs. [13,14,23], our work considers massive quasielectrons in materials such as gapped graphene. It has been reported theoretically [24] and experimentally [25] that graphene on a proper boron nitride substrate has a gap due to the breaking of sublattice symmetry. The collective excitations of the 2DEG at zero temperature ($T = 0$) are described by the linearized QHD model [18,19]

$$\frac{\partial n_{e1}}{\partial t} + n_0 \nabla \cdot \mathbf{V} = \mathbf{0}, \tag{1}$$

$$\frac{\partial \mathbf{u}_e}{\partial t} = \frac{e}{m}\nabla\phi - \frac{\pi\hbar^2}{m^2}\nabla n_{e1} + \frac{\hbar^2}{4m^2 n_0}\nabla(\nabla^2 n_{e1}), \tag{2}$$

$$\phi(\mathbf{r},t) = \int d^2\mathbf{r}' W(\mathbf{r}-\mathbf{r}') n_{e1}(\mathbf{r}',t). \tag{3}$$

Here, $\nabla = \frac{\partial}{\partial y}\mathbf{e_y} + \frac{\partial}{\partial x}\mathbf{e_x}$, $n_{e1} = n_e - n_0$ is the 2D perturbed electron density with respect to the equilibrium density n_0, m is the effective electron mass, e is the elementary charge, $\hbar$ is the Planck constant, ϕ is the electrostatic potential induced by the electron density fluctuations n_{e1}, $W(\mathbf{r}-\mathbf{r}')$ is the Coulomb interaction, and $\mathbf{u}_e$ is the normal fluid velocity. Gauss units are adopted throughout this paper without specification. The velocity field $\mathbf{V}$ includes not only the ordinary plasmon velocity $\mathbf{u}_e$ but also an additional anomalous velocity $\mathbf{V}_a$ due to the Berry flux [13],

$$\mathbf{V} = \mathbf{u}_e + \mathbf{V}_a, \quad \mathbf{V}_a = \frac{eF}{\hbar}[(\nabla\phi)\times\mathbf{e}_z]. \tag{4}$$

Here, $F = \sum_i \int d^2k \Omega_i(\mathbf{k}) f_i^0(\mathbf{k})/(2\pi)^2$ is the dimensionless Berry flux [11,13], where $f_i^0(\mathbf{k})$ is the equilibrium band i occupancy [13], and $\Omega_i(\mathbf{k})$ is the Berry curvature for band i [11]. Based on Ref. [13], we take $0 \leqslant F \leqslant 1$. Note that the final two terms on the right-hand side of Eq. (2) are regarded as QE [18,19], which are respectively the quantum statistical effect (QSE) and quantum diffraction effect (QDE) due to the Bohm force. In degenerate electron gas, the QSE comes from the Fermi-Dirac pressure due to the Pauli exclusion principle [17]. The QDE is a quantum force associated with the Bohm–de Broglie potential, which causes wave dispersion at the nanoscale [17,26]. In addition, at absolute zero temperature considered here, the damping effect is neglected in Eq. (2) due to Pauli blocking [19,27].

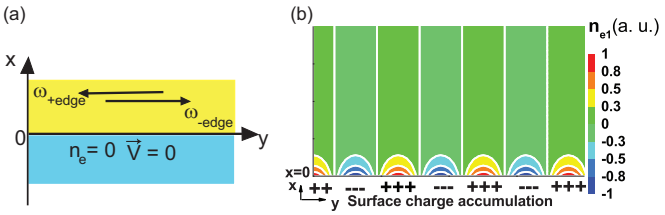

FIG. 1. (a) Schematic illustration of a metal-vacuum interface. Chiral Berry plasmons propagate along the edges of a two-dimensional metal surface with a finite Berry flux. (b) Electron density fluctuations for edge plasmons, where surface charge accumulation near the boundary $x = 0$ results from the anomalous velocity flow (white solid lines).

It is necessary to discuss the justification of Eq. (2). Based on Refs. [10,28,29], graphene has been assumed to be in the Fermi-liquid regime and is regarded as a perfect fluid, where the electron density, velocity, and pressure can be described by linearized QHD equations [19]. The QHD is derived from the Wigner-Poisson system, where the first three moments of the Wigner function integrated over the velocity space give the definitions of fluid density, velocity, and pressure. Then, the continuity and the momentum balance equations are obtained. These fluid equations are closed by the pressure term including the quantum statistical pressure and the quantum diffraction pressure term. The last term in Eq. (2) is the quantum diffraction pressure term. It originates from the Wigner distribution for a quantum mixture of states $\psi_\alpha = \sqrt{n_e}\exp(iS_\alpha/\hbar)$, where α is the occupation band, S_α is a phase related to the fluid velocity, and $\sqrt{n_e}$ is the amplitude for assuming all amplitudes are the same. The quantum diffraction pressure is obtained as $P_Q = \hbar^2/(2m)[(\nabla\sqrt{n_e})^2 - \sqrt{n_e}\nabla^2\sqrt{n_e}]$. The last term in Eq. (2) is derived in the linearized model with $n_e = n_{e1} + n_0$ and $n_{e1} \ll n_0$.

III. EDGE MODES

To illustrate the features of edge plasmons, we consider a boundary of the 2DEG at $x = 0$, as shown in Fig. 1(a). Outside the 2DEG ($x < 0$), the electron density $n_e(\mathbf{r},t)$ and total velocity $\mathbf{V}(\mathbf{r},t)$ are zero, while $n_e(\mathbf{r},t) \neq \mathbf{0}$ and $\mathbf{V}(\mathbf{r},t) \neq \mathbf{0}$ inside the 2DEG region ($x \geqslant 0$). For a given edge plasmon mode, we plot in Fig. 1(b) the surface charge accumulation near the boundary $x = 0$ which is caused by an anomalous velocity flow. For this edge plasmon propagating as a plane wave along the y axis with frequency ω and wave vector q, the potential, perturbed density, and velocity can be written as

$$\begin{aligned}
\phi(\mathbf{r},t) &= \phi_q(x)\exp(i\omega t - iqy),\\
n_{e1}(\mathbf{r},t) &= n_{e1q}(x)\exp(i\omega t - iqy),\\
u_e(\mathbf{r},t) &= u_{eq}(x)\exp(i\omega t - iqy),\\
\mathbf{V}(\mathbf{r},t) &= \mathbf{V}_q(x)\exp(i\omega t - iqy),
\end{aligned} \tag{5}$$

respectively. Accordingly, Eq. (1) becomes $n_{e1}(\mathbf{r}) = -n_0\nabla\cdot\mathbf{V}(\mathbf{r},t)/i\omega$. Further, using the steplike property of $\mathbf{V}(\mathbf{r},t)$ [$\mathbf{V}(\mathbf{r},t) \neq \mathbf{0}$ for $x \geqslant 0$ and $\mathbf{V}(\mathbf{r},t) = \mathbf{0}$ for $x < 0$], a jump

condition for the x derivative of $\phi_q(x)$ can be obtained [13], which reads

$$\left.\frac{\partial\phi_q}{\partial x}\right|_{x=0^+} - \left.\frac{\partial\phi_q}{\partial x}\right|_{x=0^-} = \frac{1}{i\omega}\left(\left.\frac{\partial W_q}{\partial x}\right|_{x=0^-} - \left.\frac{\partial W_q}{\partial x}\right|_{x=0^+}\right) n_0 \mathbf{V}_x\Big|_{x=0^+}. \quad (6)$$

Here, $\mathbf{V}_x|_{x=0^+} = \mathbf{u}_{ex}|_{x=0^+} + \mathbf{V}_{ax}|_{x=0^+}$ and $W_q = -e\int dk \exp(ikx)/\sqrt{q^2+k^2}$.

Following Refs. [2,13], we focus only on the long-wavelength limit $q \ll k_F = \sqrt{2\pi n_0}$ with k_F the Fermi wave number, where W_q can be simplified as

$$W_q(x) \approx -4\pi e \int \frac{dk}{2\pi}\frac{|q|}{k^2+2q^2}\exp(ikx) = -\frac{4\pi e}{2\sqrt{2}}\exp(-\sqrt{2}qx). \quad (7)$$

By substituting the simplified $W_q(x)$ into Eq. (3), we find

$$\phi_q(x) = \int dx' W_q(x-x') n_{e1q}(x'). \quad (8)$$

By means of the convolution theorem, we obtain a differential equation of $\phi_q(x)$ on either side of the boundary ($x = 0$),

$$\begin{aligned} &(\partial_x^2 - 2q^2)\phi_q(x) = 0, \quad x < 0, \\ &(\partial_x^2 - 2q^2)\phi_q(x) = 4\pi e|q| n_{e1q}(x), \quad x \geqslant 0. \end{aligned} \quad (9)$$

This equation has bounded solutions,

$$\begin{aligned} &\phi_q(x) = \phi_1 \exp(\kappa_1 x), \quad x < 0, \\ &\phi_q(x) = \phi_2 \exp(-\kappa_2 x), \quad x \geqslant 0, \end{aligned} \quad (10)$$

where $\kappa_1 = \sqrt{2}|q|$ and the decaying wave vector $\kappa_2 > 0$ are determined as follows. Applying $\partial/\partial t$ to the continuity relation in Eq. (1) and substituting $\frac{\partial \mathbf{V}}{\partial t} = \frac{\partial \mathbf{u_e}}{\partial t} + \frac{\partial \mathbf{V_a}}{\partial t}$ into Eq. (1), we get

$$\frac{\partial^2 n_{e1}}{\partial t^2} = -\frac{e}{m} n_0 \nabla^2\phi + \frac{\pi\hbar^2 n_0}{m^2}\nabla^2 n_{e1} - \frac{\hbar^2}{4m^2}\nabla^2(\nabla^2 n_{e1}). \quad (11)$$

Using the plane-wave forms of $n_{e1}(\mathbf{r},t)$ and $\phi(\mathbf{r},t)$ and the relation between n_{e1q} and ϕ_q in Eq. (9), we can express $n_{e1}(\mathbf{r},t)$ on the 2DEG side ($x \geqslant 0$) as

$$n_{e1}(\mathbf{r},t) = \frac{\phi_2}{4\pi e|q|}(\kappa_2^2 - 2q^2)e^{-\kappa_2 x}e^{i\omega t - iqy}. \quad (12)$$

Substituting this expression into Eq. (11) we yield

$$1 = \frac{2\omega_P^2(q)}{\omega^2}\frac{\kappa_2^2 - q^2}{\kappa_2^2 - 2q^2} - A_S\frac{\kappa_2^2 - q^2}{\omega^2} + A_D\frac{(\kappa_2^2 - q^2)^2}{\omega^2}, \quad (13)$$

where $\omega_P(q) = \sqrt{2\pi n_0 e^2|q|/m}$ is the bulk plasmon frequency [2] without QE and Berry flux, and $A_S = \pi\hbar^2 n_0/m^2$ and $A_D = \hbar^2/4m^2$ are the coefficients of the QSE- and QDE-related terms.

To determine the dispersion relation of edge plasmons we need another equation derived from the continuity condition of ϕ and the jump boundary condition Eq. (6),

$$\begin{aligned} &\sqrt{2}|q| + \kappa_2 \\ &= \frac{2\omega_p^2(q)}{\omega^2}\kappa_2 - A_F\frac{q^2\,\mathrm{sgn}(q)}{\omega} \\ &\quad - A_Q\frac{\kappa_2(\kappa_2^2 - 2q^2)}{\omega^2} + A_D\frac{\kappa_2(\kappa_2^2 - 2q^2)(\kappa_2^2 - q^2)}{\omega^2}. \end{aligned} \quad (14)$$

Here, $A_F = 4\pi e^2 F/\hbar$ is the coefficient of the chiral Berry term. The two coupled nonlinear equations, Eqs. (13) and (14), are solved semianalytically to obtain the decaying wave vector κ_2 and frequency ω for a given wave vector q. From Eq. (14) one can see that the dispersion relation of edge plasmons depends on the propagating direction. We denote the frequency of forward-propagating (backward-propagating) edge modes with $q > 0$ ($q < 0$) as $\omega_{-\mathrm{edge}}$ ($\omega_{+\mathrm{edge}}$). Without QE, $\omega_{+\mathrm{edge}}$ has a faster propagation than $\omega_{-\mathrm{edge}}$ and merges with the bulk plasmon at a threshold frequency [13].

We can obtain the limits of both ω and κ_2 for $q \to 0^-$ and $q \to 0^+$ for a finite A_F,

$$\begin{aligned} &\kappa_2|q \to 0^- = O(q^4), \\ &\omega|q \to 0^- = 2.1\omega_p^2/(A_F|q|), \\ &\kappa_2|q \to 0^+ = 0.7q, \\ &\omega|q \to 0^+ = 0.35A_F q. \end{aligned} \quad (15)$$

Without QE or $A_F = 0$, one has the long-wavelength limit $\omega|q \to 0 = \sqrt{2/3}\omega_p(q)$. Therefore, the QE in CBPs with a finite Berry flux turns the bidirectional acoustic edge plasmon into a unidirectional one. Note that the propagating velocity of unidirectional edge modes depends only on the Berry flux through A_F. The difference in long-wavelength limits for the two propagating directions arises from the singularity of nonlinear Eqs. (13) and (14) at $q = 0$.

For a two-dimensional bulk plasmon with perturbed electron density $n_{e1} \sim \exp(i\omega t - i\mathbf{q}\cdot\mathbf{r})$, the dispersion relation derived from Eqs. (1)–(3) reads $\omega_q(\mathrm{bulk})^2 = \omega_P^2(q) + A_S q^2 + A_D q^4$. In the considered range of wave vector, there is only a tiny difference between $\omega_q(\mathrm{bulk})$ and $\omega_P(q)$.

IV. RESULTS AND DISCUSSION

In the following, we present the semianalytical solutions of Eqs. (13) and (14), where the MATLAB solver function is used to solve the two coupled transcendental equations. The electron density in equilibrium and the effective mass are taken to be the same as in Ref. [13], $n_0 = 6\times10^{10}\,\mathrm{cm}^{-2}$ and $m = 0.03m_e$ as measured in graphene [30], with m_e the free-electron mass. The plasmon frequency ω is in units of $E_F/\hbar$ with $E_F = \hbar^2 k_F^2/2m$ the Fermi energy.

In Fig. 2(a), the dispersion relations of edge plasmons in the presence/absence of QE are plotted as curves with triangles/circles. The dimensionless Berry flux is set at $F = 1$. Without the QE, acoustic edge plasmons appear in the long-wavelength limit and exhibit a direction-dependent dispersion (i.e., the chirality). This behavior agrees with that in Ref. [13]. The $\omega_{+\mathrm{edge}}$ acoustic mode has a threshold frequency ω_{th} at which it merges with the bulk plasmon mode. We find

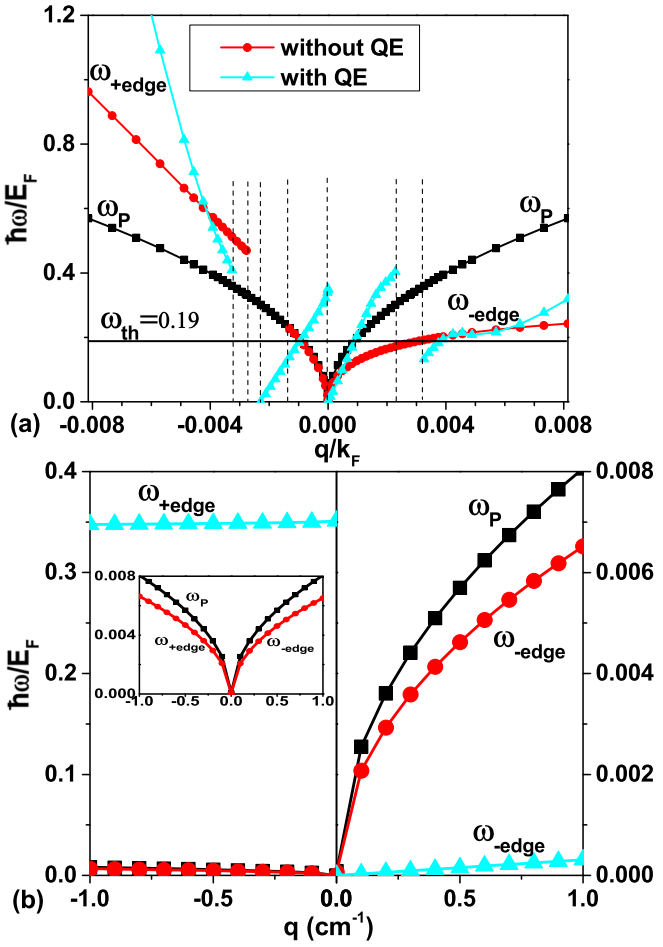

FIG. 2. (a) Dispersion of edge plasmons without (circles) and with (triangles) the quantum effect (QE), compared to bulk plasmon dispersion $\omega_P(q)$ (squares). (b) Zoom-in of the dispersion near $q = 0$. Note that different frequency scales are used in the left and right panels. The inset in (b) shows ω_P and $\omega_{\pm\text{edge}}$ without the QE near $q = 0$. The dimensionless Berry flux is fixed at $F = 1$.

that above $\omega_{\text{th}0}$ and for $q < -0.0028k_F$ the $\omega_{+\text{edge}}$ mode reappears, with a frequency notably higher than $\omega_P(q)$. Such a mode cannot be obtained in the first-order q approximation ($A_F q \ll \omega_P$) in Ref. [13]. When the QE is considered, the acoustic edge plasmon mode exists only for $q > 0$. The $\omega_{+\text{edge}}$ mode has a maximum frequency in the vicinity of $q = 0$, and decreases with increasing $|q|$ for $|q|/k_F \leqslant 0.0024$. Both $\omega_{+\text{edge}}$ and $\omega_{-\text{edge}}$ dispersion curves intersect the bulk plasmon dispersion at the threshold frequency $\omega_{\text{th}} = 0.19E_F/\hbar$ and $q/k_F = \pm 9.77 \times 10^{-4}$ and have a frequency gap within $0.0024 < |q|/k_F \leqslant 0.0033$.

The dispersion curves near $q = 0$ are shown more clearly in Fig. 2(b), which confirms the limit behaviors in Eq. (15). Without the QE, $\omega_{+\text{edge}}$ and $\omega_{-\text{edge}}$ are symmetric in the vicinity of $q = 0$ with a $\sqrt{|q|}$ dependence and tend to ω_P at $q = 0$ (see the inset). In the presence of QE, the one-way acoustic edge mode $\omega_{-\text{edge}}$ has a linear dispersion rather than a $\sqrt{|q|}$ dependence. This one-way edge plasmon mode is caused by the QE and Berry flux, which presents some similar characters with the one-way edge magnetoplasmon mode reported in Ref. [5]. The $\omega_{+\text{edge}}$ is constant in the considered q range. The chirality is manifested in the splittings of the $\omega_{\pm\text{edge}}$ mode for counterpropagating edge plasmons near $q = 0$. Such splittings have potential applications in subwavelength optical nonreciprocity [15].

The transverse confinements of these edge plasmon modes are shown in Fig. 3 under the same parameters as in Fig. 2. Without the QE, the ratio $|q|/\kappa_2$ for the acoustic edge mode $\omega_{+\text{edge}}$ increases with $|q|$ and diverges at $q/k_F = -0.0013$. In contrast, for the mode $\omega_{-\text{edge}}$, the ratio $|q|/\kappa_2$ decreases with $|q|$ and tends to a constant. The presence of the QE enhances the transverse confinement of the $\omega_{-\text{edge}}$ acoustic mode for $q/k_F > 4.9 \times 10^{-4}$. For the $\omega_{+\text{edge}}$ mode, the ratio $|q|/\kappa_2$ is divergent at $q = 0^-$ and decreases quickly with increasing $|q|$. In the frequency range $[0,\omega_{\text{th}}]$, the $\omega_{+\text{edge}}$ mode has a strong confinement. These features can be ascribed to the coupling of the quantum terms and the chiral term shown in the following equation for a finite A_F,

$$\begin{aligned}\omega = {} & \omega_P^2\left(-2.1 + \kappa_2/|q| + \kappa_2^2/q^2\right)/(A_F q) \\ & + A_F\left(0.35q^2 - 0.35\kappa_2^2\right)/q \\ & + A_S\left(-0.7\kappa_2^4/q^2 - \kappa_2^3/|q| + 1.3\kappa_2^2\right. \\ & \left. + \kappa_2|q| - 2.1q^2\right)/(A_F q) \\ & + A_D\left(0.7\kappa_2^6/q^2 + \kappa_2^5/|q| - 3.2\kappa_2^4 - 3\kappa_2^3|q|\right. \\ & \left. + 4.6\kappa_2^2 q^2 + 2\kappa_2 q^2|q| - 2.1q^4\right)/(A_F q). \end{aligned} \quad (16)$$

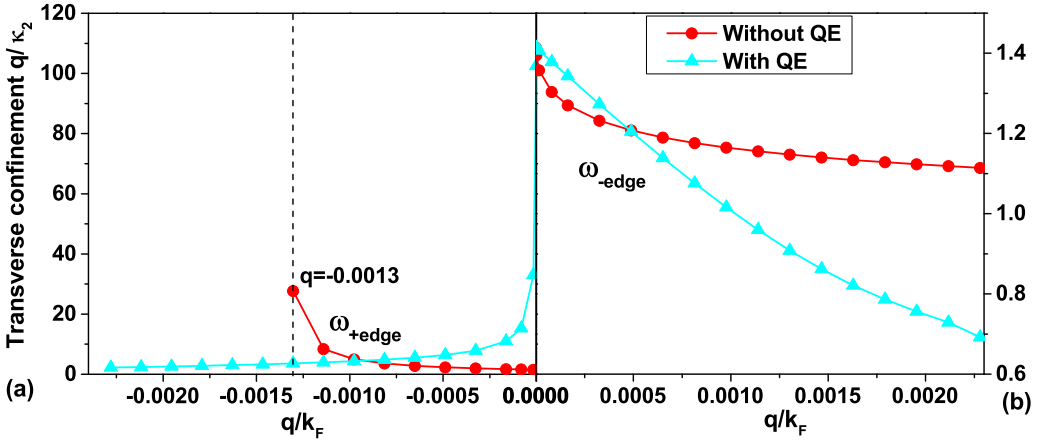

FIG. 3. Transverse confinement length of an edge plasmon expressed as $|q|/\kappa_2$ for (a) $\omega_{+\text{edge}}$ and (b) $\omega_{-\text{edge}}$ modes, without and with QE.

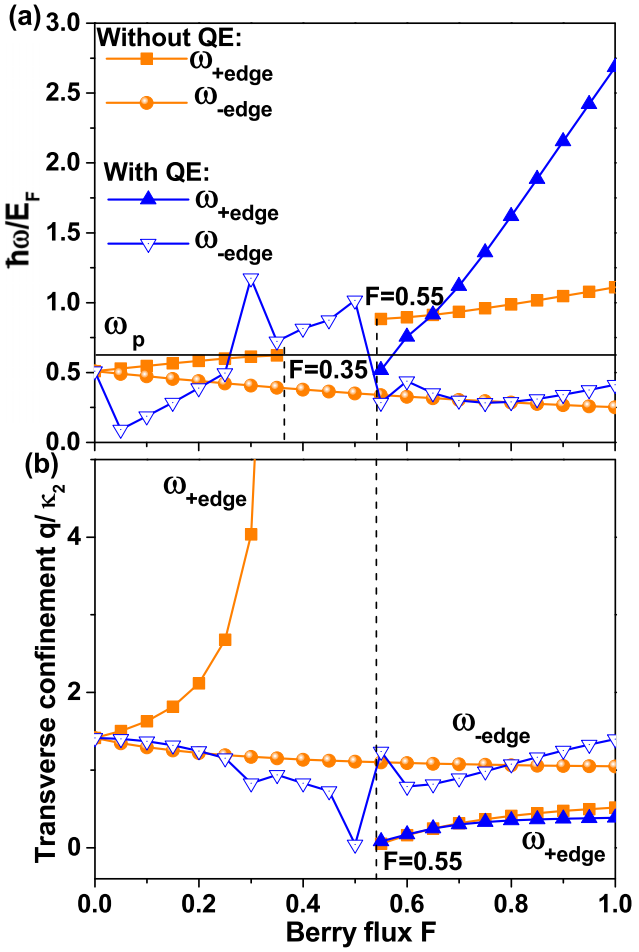

FIG. 4. (a) Frequency and (b) transverse confinement length of edge plasmons as functions of the dimensionless Berry flux F, without and with QE. The transverse confinement length is expressed as $|q|/\kappa_2$. $|q|/k_F$ is fixed at 0.0098.

This expression is regarded as a semianalytic dispersion relation, where κ_2 is determined from the solutions of two coupled polynomial functions of the fourth and fifth orders [Eqs. (13) and (14)]. The significantly enhanced transverse localization is preferable for the realization of subwavelength optical nonreciprocal devices in the THz range with no magnetic field.

To demonstrate the effect of Berry flux F on the edge plasmons, we plot in Fig. 4 the variation of frequency $\omega_{\pm\text{edge}}$ and transverse confinement length $|q|/\kappa_2$ as a function of F. The wave vector is fixed at $q/k_F = \pm 0.0098$. Without the QE, the splitting $\omega_{\pm\text{edge}}$ modes and their confinement length agree well with those in Ref. [13], expect for the reappearance of $\omega_{+\text{edge}}$ for $F \geqslant 0.55$. This $\omega_{+\text{edge}}$ mode is a nonlinear solution of Eqs. (13) and (14). Its frequency and confinement length increase with F. Note that this $\omega_{+\text{edge}}$ mode has a stronger confinement than the corresponding $\omega_{-\text{edge}}$ mode. When the QE turns on, $\omega_{+\text{edge}}$ vanishes for $F < 0.55$ while $\omega_{-\text{edge}}$ shows an oscillation (around the curve without QE) in both the frequency and the confinement length. The complicated features can be seen from Eq. (16), where the frequency is a polynomial of the decay constant κ_2 with F-dependent coefficients.

Finally, we compare the chiral edge plasmons under the QE with the MPs. Fetter [2] has investigated the MPs based on a conventional hydrodynamic model. It was found that the classical statistical pressure term with strength $\propto sq$ has almost no effect on the edge modes in the limit $sq \ll \omega_P$, where $s^2 = m^{-1}(\partial p/\partial n)$. In the QHD model, the effect of the conventional pressure term becomes the QE including the QSE and QDE. The QE changes greatly the features of the edge modes, even in the limit $sq \ll \omega_P$ (which becomes $A_Q q^2 \ll \omega_P^2$ and $A_D q^4 \ll \omega_P^2$ in the present work). The relative importance of QE for a degenerate case is represented by the dimensionless quantum coupling parameter, which is the ratio of the potential energy and the kinetic energy $\Gamma_Q \sim \hbar\omega_P/E_F$ [19,20], where k_B is the Boltzmann constant.

In the degenerate case considered here, the typical kinetic energy of a particle is on the order of the Fermi energy and is almost temperature independent [17]. Thus the quantum coupling parameter is immune from the temperature effect. The results presented in this work are not changed by finite temperature effects in the degenerate case. The more electrons are occupied in a fixed region, the more their wave functions are restricted. This indicates that a high electron density will lead to the enhancement of the Fermi pressure due to the exclusion principle. When the density is high enough, $\Gamma_Q \sim 1$, corresponding to a Landau length comparable to the de Broglie wavelength. In this case the QE is expected to appear [19,20]. There are two points why the classical state and quantum state differ significantly. First, the quantum statistical pressure ($\Gamma_Q \sim 1$ and $\hbar \neq 0$) is distinct from the classical statistical pressure ($\Gamma_Q \to 0$ and $\hbar \to 0$), because the phase-space representatives of the quantum states are more restricted than those of the classical state [31–33]. Second, the QDE is responsible for quantum tunneling, which is a pure quantum effect absent in classical statistical pressure [20].

V. EXPERIMENTAL REALIZATION

In gapped Dirac materials, a pumping with circularly polarized light can generate a nonzero net Berry flux [13]. The finite Berry flux yields a chiral Berry edge plasmon as shown in Fig. 1(b). When the QE is added to this chiral Berry edge plasmon, the bidirectional acoustic edge plasmon transmits to the unidirectional one. These one-way chiral edge modes without magnetic fields propose different paradigms for realizing optical nonreciprocity in the terahertz range [15]. An edge plasmon mode has been determined by optical absorption [13,34]. Near-field techniques [34], such as photon scanning tunneling microscopy (PSTM), can be employed to measure the optical absorption on a metal surface. PSTM is employed to scan the near-field optical microscope and map the near-field intensities with the sample grown on a glass prism. Prism coupling has been used to enhance the momentum of incident light [35]. Barnes *et al.* have predicted that the surface plasmon dispersion relation can be directly imaged using a modified prism coupling technique [34], where both the band gap (indicated by a dark region) and the edge plasmon region (more intensive light) can be seen in the optical absorption image. This technique can be used to experimentally reveal the existence of different one-way chiral edge modes with an energy gap, obtained in this theoretical work. Therefore, we

conclude that the phenomena discussed in this work are within experimental accessibility.

VI. CONCLUSIONS

In summary, we have adopted a quantum hydrodynamic theory to study chiral edge plasmons in a two-dimensional electron gas with a finite Berry flux. The transverse decay length and the edge plasmon frequency are obtained by nonlinearly and semianalytically solving two coupled transcendental equations. The presence of QE alters greatly the dispersion and the transverse confinement of edge plasmons. The acoustic edge plasmons propagate unidirectionally and can have a stronger transverse confinement. The QE also leads to frequency gaps for edge plasmons propagating in either direction. The edge plasmon modes exhibit different long-wavelength limits for forward- and backward-propagating directions, which is in contrast to the case without the QE. These one-way chiral edge modes without magnetic field will elucidate different paradigms for realizing optical nonreciprocity in the terahertz range, avoiding the current requirement for large magnetic-based devices.

ACKNOWLEDGMENT

This work was supported by National Natural Science Foundation of China (NSFC) (11405067, 11375163, and 11575135).

[1] D. B. Mast, A. J. Dahm, and A. L. Fetter, Phys. Rev. Lett. **54**, 1706 (1985).
[2] A. L. Fetter, Phys. Rev. B **32**, 7676 (1985).
[3] I. L. Aleiner and L. I. Glazman, Phys. Rev. Lett. **72**, 2935 (1994).
[4] N. Kumada, P. Roulleau, B. Roche, M. Hashisaka, H. Hibino, I. Petković, and D. C. Glattli, Phys. Rev. Lett. **113**, 266601 (2014).
[5] D. Jin, L. Lu, Z. Wang, C. Fang, J. D. Joannopoulos, M. Soljačić, L. Fu, and N. X. Fang, Nat. Commun. **7**, 13486 (2016).
[6] C. A. Downing and G. Weick, Phys. Rev. B **95**, 125426 (2017).
[7] Z. Fei, M. Goldflam, J.-S. Wu, S. Dai, M. Wagner, A. McLeod, M. Liu, K. Post, S. Zhu, G. Janssen *et al.*, Nano Lett. **15**, 8271 (2015).
[8] A. Nikitin, P. Alonso-González, S. Vélez, S. Mastel, A. Centeno, A. Pesquera, A. Zurutuza, F. Casanova, L. Hueso, F. Koppens *et al.*, Nat. Photonics **10**, 239 (2016).
[9] D. Rodrigo, O. Limaj, D. Janner, D. Etezadi, F. J. G. de Abajo, V. Pruneri, and H. Altug, Science **349**, 165 (2015).
[10] A. Principi, M. I. Katsnelson, and G. Vignale, Phys. Rev. Lett. **117**, 196803 (2016).
[11] D. Xiao, W. Yao, and Q. Niu, Phys. Rev. Lett. **99**, 236809 (2007).
[12] D. Xiao, G.-B. Liu, W. Feng, X. Xu, and W. Yao, Phys. Rev. Lett. **108**, 196802 (2012).
[13] J. C. Song and M. S. Rudner, Proc. Natl. Acad. Sci. USA **113**, 4658 (2016).
[14] A. Kumar, A. Nemilentsau, K. H. Fung, G. Hanson, N. X. Fang, and T. Low, Phys. Rev. B **93**, 041413 (2016).
[15] D. L. Sounas, C. Caloz, and A. Alu, Nat. Commun. **4**, 2407 (2013).
[16] D. Jalas, A. Petrov, M. Eich, W. Freude, S. Fan, Z. Yu, R. Baets, M. Popovic, A. Melloni, J. D. Joannopoulos *et al.*, Nat. Photonics **7**, 579 (2013).
[17] F. Haas, *Quantum Plasmas: An Hydrodynamic Approach* (Springer, Berlin, 2011).
[18] F. Haas, G. Manfredi, and M. Feix, Phys. Rev. E **62**, 2763 (2000).
[19] G. Manfredi and F. Haas, Phys. Rev. B **64**, 075316 (2001).
[20] L. Garcia, F. Haas, L. de Oliveira, and J. Goedert, Phys. Plasmas **12**, 012302 (2005).
[21] M. Marklund and G. Brodin, Phys. Rev. Lett. **98**, 025001 (2007).
[22] J. A. Frenje, P. E. Grabowski, C. K. Li, F. H. Séguin, A. B. Zylstra, M. Gatu Johnson, R. D. Petrasso, V. Y. Glebov, and T. C. Sangster, Phys. Rev. Lett. **115**, 205001 (2015).
[23] R. Gorbachev, J. Song, G. Yu, A. Kretinin, F. Withers, Y. Cao, A. Mishchenko, I. Grigorieva, K. Novoselov, L. Levitov *et al.*, Science **346**, 448 (2014).
[24] G. Giovannetti, P. A. Khomyakov, G. Brocks, P. J. Kelly, and J. van den Brink, Phys. Rev. B **76**, 073103 (2007).
[25] E. Wang, X. Lu, S. Ding, W. Yao, M. Yan, G. Wan, K. Deng, S. Wang, G. Chen, L. Ma *et al.*, Nat. Phys. **12**, 1111 (2016).
[26] P. Shukla, Phys. Lett. A **352**, 242 (2006).
[27] N. W. Ashcroft and N. D. Mermin, *Solid State Physics* (Holt, Rinehart and Winston, New York, 1976).
[28] G. Giuliani and G. Vignale, *Quantum Theory of the Electron Liquid* (Cambridge University Press, Cambridge, UK, 2005).
[29] M. Müller, J. Schmalian, and L. Fritz, Phys. Rev. Lett. **103**, 025301 (2009).
[30] H. Yoon, C. Forsythe, L. Wang, N. Tombros, K. Watanabe, T. Taniguchi, J. Hone, P. Kim, and D. Ham, Nat. Nanotechnol. **9**, 594 (2014).
[31] E. Wigner, Phys. Rev. **40**, 749 (1932).
[32] P. Kasperkovitz and M. Peev, Phys. Rev. Lett. **75**, 990 (1995).
[33] G. Manfredi and M. R. Feix, Phys. Rev. E **53**, 6460 (1996).
[34] W. L. Barnes, A. Dereux, and T. W. Ebbesen, Nature (London) **424**, 824 (2003).
[35] E. Kretschmann and H. Raether, Z. Naturforsch., A **23**, 2135 (1968).